Synthesis, Characterization, and Ligand Substitution of $[HFe_4(CO)_{12}BH]^-$: An Isoelectronic and Isoprotonic Inorganometallic Analogue of $HFe_4(CO)_{12}CH$

Catherine E. Housecroft,† Margaret L. Buhl,‡ Gary J. Long,‡ and Thomas P. Fehlner*†

Contribution from the Departments of Chemistry, University of Notre Dame, Notre Dame, Indiana 46556, and University of Missouri—Rolla, Rolla, Missouri 65401.
Received October 20, 1986

Abstract: The anion $[HFe_4(CO)_{12}BH]^-$ has been prepared by the deprotonation of $HFe_4(CO)_{12}BH_2$ and by the reaction of $[HFe_3(CO)_9BH_3]^-$ with $Fe_2(CO)_9$. The latter constitutes an example of a high yield cluster expansion reaction that occurs with the concurrent production of $Fe(CO)_5$ and H_2. The most stable hydrogen locations on $[HFe_4(CO)_{12}BH]^-$ are analogous to those on the isoelectronic $HFe_4(CO)_{12}CH$ molecule; however, hydrogen mobility on the cluster framework is more facile for the ferraborane than for the hydrocarbon analogue. Substitution of CO by $PPhMe_2$ on $[HFe_4(CO)_{12}BH]^-$ occurs cleanly on a "wing-tip" iron via a second-order process involving a transient intermediate containing $PPhMe_2$. Endo-hydrogen position is unaffected by monosubstitution, but the energy barrier associated with hydrogen exchange is increased. Replacement of a second CO by phosphine on the other "wing-tip" iron proceeds more slowly and results in the conversion of the FeHFe into a FeHB interaction, thereby producing a coordinated BH_2 fragment. The effects that B^-/C and $CO/PPhMe_2$ interchanges have on stable hydrogen position and on endo-hydrogen mobilities are discussed within the framework of extended Hückel calculations.

Under appropriate conditions, both orbitally rich ("electron deficient") main-group and transition-metal atoms condense into three-dimensional clusters.[1] Besides forming homonuclear clusters, the main-group atom is found as a constituent of terminal or bridging ligands and is partially, or sometimes even totally, incorporated into a transition-metal cluster as a part of the cluster framework or as an interstitial atom.[2] No matter what the mode of interaction with the transition metal, the main-group atom modifies the metal structure and chemistry and, in the process, is itself modified. Just as the organic chemist is interested in the nature of the organic moiety in an organometallic compound, so too, we are interested in knowing how the chemistry of a main-group fragment is changed by virtue of its interaction with transition metals in "inorganometallic" compounds. In this paper we describe the synthesis of $[HFe_4(CO)_{12}BH]^-$ (II), by routes including cluster expansion[3] and define the stable endo-hydrogen position and mobility as a function of the substituents on the metal.[4] As II is isoelectronic and isoprotonic with $HFe_4(CO)_{12}CH$[5] (IV), it also provides an opportunity to directly compare selected properties of the inorgano- and organometal analogues. We are particularly interested in factors that control stable endo-hydrogen location and hydrogen mobility over the cluster framework.

Synthesis of $[HFe_4(CO)_{12}BH]^-$ by Cluster Expansion. Cluster expansion reactions are now well-known;[6] however, examples proceeding in high yield with clean, well-defined stoichiometry are scarce. Operating from the impetus of theoretical modeling results[7] as well as experimental precedent,[8] we investigated the products and stoichiometry of the reaction of III in a solvent with solid $Fe_2(CO)_9$. The non-boron-containing products are H_2 and $Fe(CO)_5$, which were identified by gas–liquid chromatography and infrared spectroscopy, respectively. The conversion of III to a single boron-containing product is revealed by the ^{11}B NMR spectra shown in Figure 1 where we note that the yield of II is quantitative by NMR. The anionic ferraborane product has been characterized as II, as follows. Protonation of II with CF_3COOH yields $HFe_4(CO)_{12}BH_2$[9] (I), (quantitatively by NMR). The infrared spectrum of II in the carbonyl region exhibits a pattern of bands similar to that of I except that it is shifted about 50 cm^{-1} to lower energy (Figure 2). In addition, a distinctive band at 808 cm^{-1}, not due to PPN, is assigned to the skeletal vibrations[10] of the "interstitial" boron atom of II. This suggests that the metal framework of the anion is the same as that of I; i.e., no skeletal rearrangement has taken place.

Chart I

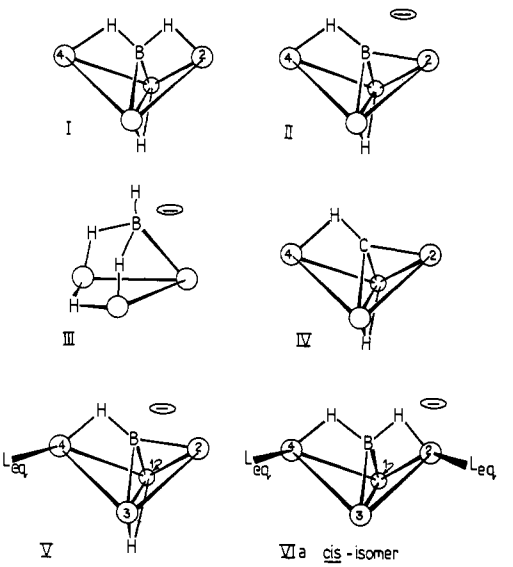

Table I. Mössbauer Effect Spectral Parameters[a] for $[PPN][HFe_4(CO)_{12}BH]$[b]

component	δ	ΔE_Q	Γ	% A
outer Fe(2)	−0.06	1.86	0.20	8.0
middle Fe(4)	−0.03	1.06	0.38	26.1
inner Fe(1)(3)	−0.03	0.65	0.44	61.4

[a] Data obtained at 78 K and given in mm/s relative to room-temperature natural abundance α-iron foil. [b] A doublet at ~0.8 mm s^{-1} and fit to 4.5% of the absorption is ascribed to an impurity.

† University of Notre Dame.
‡ University of Missouri—Rolla.

(1) Greenwood, N. N.; Earnshaw, A. *Chemistry of the Elements*; Pergamon: New York, 1984.
(2) Johnson, B. F. G., Ed. *Transition Metal Clusters*; Wiley: New York, 1980.
(3) Housecroft, C. E.; Fehlner, T. P. *Organometallics* **1986**, *5*, 379.
(4) Housecroft, C. E.; Fehlner, T. P. *Organometallics* **1986**, *5*, 1279.
(5) Beno, M. A.; Williams, J. M.; Tachikawa, M.; Muetterties, E. L. *J. Am. Chem. Soc.* **1981**, *103*, 1485.
(6) Vahrenkamp, H. *Adv. Organomet. Chem.* **1983**, *22*, 169.

0002-7863/87/1509-3323$01.50/0

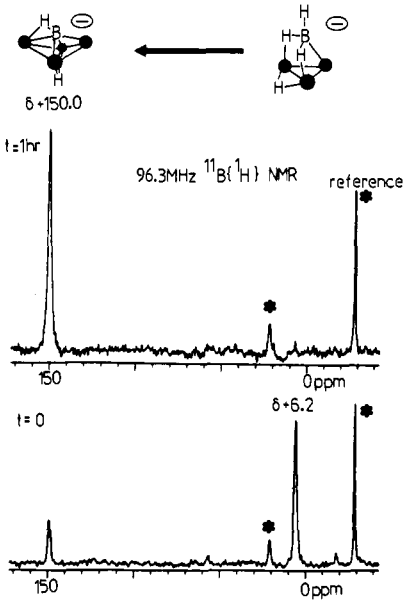

Figure 1. ^{11}B NMR spectra of the reaction of III with $Fe_2(CO)_9$ in acetone at 25 °C. The resonances with asterisks are in the external reference.

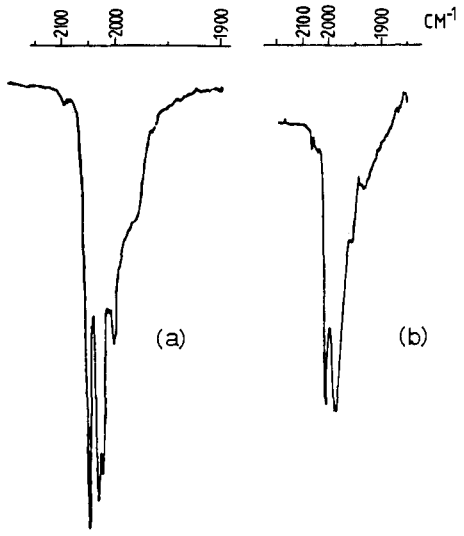

Figure 2. Infrared spectra of (a) I (hexane) and (b) [II]PPN (toluene) in the carbonyl region.

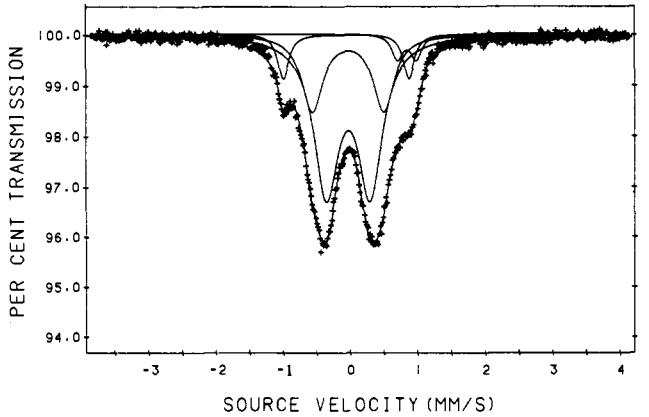

Figure 3. Mössbauer spectrum of [II]PPN obtained at 78 K.

The Mössbauer spectrum shown in Figure 3, and the spectral parameters in Table I are consistent with this conclusion. Because

(7) Fehlner, T. P.; Housecroft, C. E. *Organometallics* **1984**, *3*, 764.

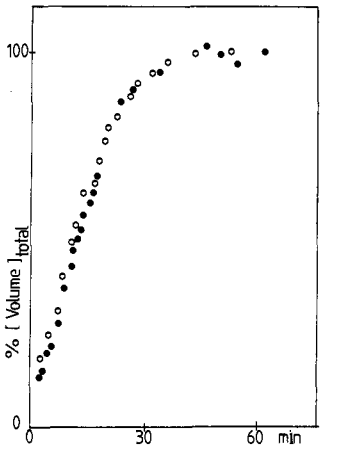

Figure 4. Volume of gas produced in reaction 2 in toluene at 25 °C and 1 atm for open circles, 0.012 mmol of III with 0.063 mmol of $Fe_2(CO)_9$ producing 0.012 mmol of gas at 60 min, and for closed circles, 0.054 mmol of III with an excess (unmeasured) of $Fe_2(CO)_9$ producing 0.055 mmol of gas at 60 min.

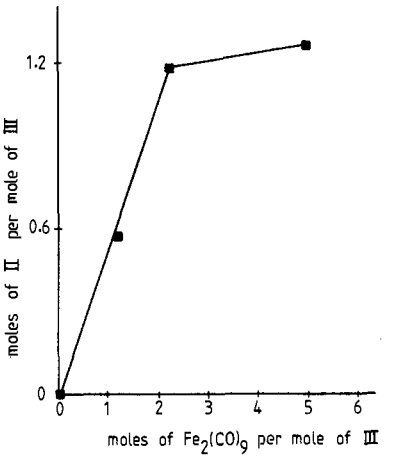

Figure 5. A plot of the ratio of the final ^{11}B NMR integral of II to the initial integral of III as a function of moles of $Fe_2(CO)_9$ added per mole of III.

II is isoelectronic with IV, the Mössbauer spectrum provides another test of structure.[11] The observed spectrum (Figure 3) requires four symmetric quadrupole doublets to obtain a satisfactory fit. As an Fe(III) impurity of about 5% constitutes one of the doublets, II exhibits three distinct iron sites in accord with the proposed structure in Chart I. The outer doublet with the lowest isomer shift has been assigned to Fe(2) reflecting the negative charge associated with this "wing-tip" iron. The inner doublet, having the largest area, has been assigned to the two equivalent irons Fe(1) and (3). Finally, the middle doublet is assigned to Fe(4). The similar isomer shifts of Fe(1), Fe(3), and Fe(4) indicate similar s-electron densities; however, the quadrupole interactions are considerably different. Although the quadrupole interactions at the hinge iron sites and Fe(2) are similar in both II and the carbide IV,[11] the Fe(4) site has a significantly larger quadrupole splitting, and hence a larger electric field gradient at the iron nucleus, than that of the equivalent iron site in IV. Possibly this lower symmetry is a result of a stronger Fe(4)–H interaction in II as compared to that in IV. This would be con-

(8) Vahrenkamp, H. In *Transition Metal Chemistry*; Mueller, A., Diemann, E., Eds.; Verlag Chemie: Basel, 1981; p 35.
(9) Wong, K. S.; Scheidt, W. R.; Fehlner, T. P. *J. Am. Chem. Soc.* **1982**, *104*, 1111.
(10) Johnson, B. F. G.; Lewis, J.; Nelson, W. J. H.; Nicholls, J. N.; Vargas, M. D. *J. Organomet. Chem.* **1983**, *249*, 255.
(11) The Mössbauer spectrum of IV has been reported: Benson, C. G.; Long, G. J.; Bradley, J. S.; Kolis, J. W.; Shriver, D. F. *J. Am. Chem. Soc.* **1986**, *108*, 1898.

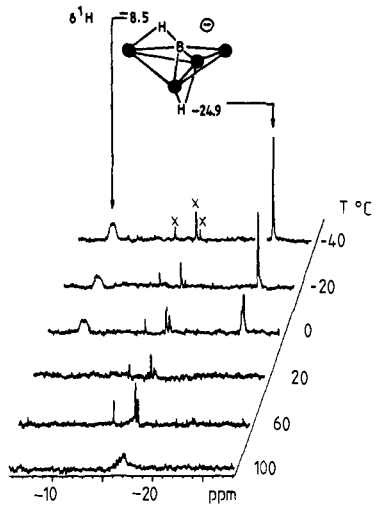

Figure 6. Variable-temperature ^1H NMR spectra of II in $(CD_3)_2CO$ ($T \leq 20$ °C) and in $C_6D_5CD_3$ ($T > 20$ °C). The resonances marked with ×'s are known impurities that decompose at high temperature.

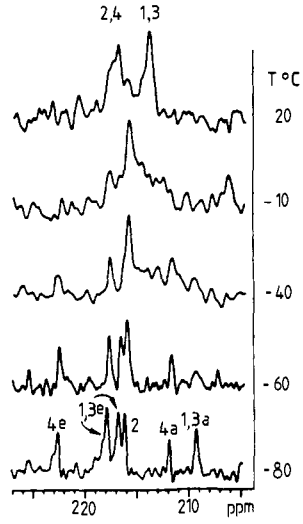

Figure 7. Natural abundance variable-temperature ^{13}C NMR spectrum of II in CH_2Cl_2. Nomenclature is given in Chart II.

sistent with the bonding picture derived from the NMR results discussed below. Although the specific assignments given in Table I are tentative, the Mössbauer spectra clearly indicate the presence of three chemically different iron sites in II.

The cluster expansion reaction of III to II proceeds via the stoichiometry expressed in reaction 1. The gas evolved was

$$[HFe_3(CO)_9BH_3]^- + 2Fe_2(CO)_9 \rightarrow [HFe_4(CO)_{12}BH]^- + H_2 + 3Fe(CO)_5 \quad (1)$$

measured volumetrically as a function of time[13] with the composition of the gas produced being measured by gas chromatography. When either stoichiometric quantities of $Fe_2(CO)_9$ or else an excess $Fe_2(CO)_9$ with reaction times shorter than 40 min was used, the gas produced consisted of only H_2. The gas production for two different reactant ratios is shown in Figure 4. Consistent with the insolubility of $Fe_2(CO)_9$ in toluene, the reaction is zero-order in $Fe_2(CO)_9$. Quantitative infrared spectroscopy was used to define the stoichiometry with respect to $Fe(CO)_5$. Finally, as shown in Figure 5, a "titration" of III with $Fe_2(CO)_9$ defines the stoichiometry with respect to $Fe_2(CO)_9$. Additional experiments have shown that large excesses of $Fe_2(CO)_9$ and reaction times greater than 1 h result in reduced yields of II as measured by ^{11}B NMR. Under these conditions, CO, $[HFe_3(CO)_{11}]^-$, and $Fe_3(CO)_{12}$ were observed as additional products.

An important characteristic of reaction 1 is the elimination of H_2. We have already shown that III undergoes substitution with certain Lewis bases via H_2 elimination rather than CO displacement.[14] The electrons contributed by the two endo hydrogens are replaced by the pair provided by the base. Formation of II from III results in the two electrons of the endo hydrogens being formally replaced by the pair of electrons from the $Fe(CO)_3$ fragment. A test of the importance of these endo hydrogens results from an examination of the ferraborane $[Fe_3(CO)_9(\mu\text{-}CO)BH_2]^-$,[15] which contains only a single endo hydrogen. This anion does not react with $Fe_2(CO)_9$ under the conditions stipulated above. On the other hand, $HFe_3(CO)_9(\mu\text{-}CO)BH_2$, which contains two endo hydrogens, does react to yield yet uncharacterized products.[16] Thus, the elimination of the two endo hydrogens from III constitutes one driving force for the reaction.

The implications of the formation of $Fe(CO)_5$ rather than CO or $Fe_3(CO)_{12}$ in reaction 1 are not fully understood. Consideration of the heats of formation of CO, $Fe(CO)_5$, and $Fe_3(CO)_{12}$ shows that reaction 1 is favored over reaction 2 by 25 kcal/mol. On

$$[HFe_3(CO)_9BH_3]^- + 2Fe_2(CO)_9 \rightarrow [HFe_4(CO)_{12}BH]^- + H_2 + 3CO + Fe_3(CO)_{12} \quad (2)$$

the other hand, the formation of CO as a volatile gas must be entropically favored over the formation of $Fe(CO)_5$. Thus, the role of $Fe(CO)_5$ as the preferred vehicle for CO removal may also be mechanistically significant and deserves further investigation.

Fluxional Behavior. The variable-temperature ^1H NMR spectra of II shown in Figure 6 demonstrate that the FeHB and FeHFe protons exchange rapidly on the NMR time scale at temperatures above 60 °C. Higher temperatures are required to effect the same exchange in the carbon analogue IV;[17] i.e., the mobility of the endo hydrogens is greater in the boron anion than in the carbon compound. Both compounds have the same relative, stable proton locations, but the geometry of the FeHE (E = C, B) interaction is skewed toward carbon;[5,9] i.e., the FeB and FeC distances are nearly equal, but the CH distance is less than the BH distance. This suggests that the stronger CH interaction reduces the mobility of the hydrogens on the metal framework.

The variable-temperature ^{13}C NMR spectra of II are shown in Figure 7. At the highest temperature examined, two signals are seen in a 1:1 ratio, one of which is still broad. The reported ^{13}C NMR of IV demonstrates intramolecular CO exchange restricted to individual iron sites.[5] The same is reasonable in II. As only two resonances are observed, a rapid H exchange process at this temperature is required to make the butterfly "wing-tips" equivalent on the NMR time scale. Just such a process has been described in the discussion of the proton spectrum above. Hence, the observed two resonances are assigned to "wing-tip" and "hinge" CO's. At −90 °C six CO signals are evident requiring H motions to be frozen out at this temperature. That is, if the H's are fluxional only four types of CO would be observed. However, the static structure II should exhibit seven CO resonances. The fact that six are observed suggests that intrametal site exchange is frozen out at the equivalent "hinge" sites but at only one of the "wing-tip" sites.

Although sufficient information is not available for an unambiguous assignment of the low-temperature spectrum, a reasonable one follows. Using the observations on IV[5] as a guide, we assume that axial "hinge" CO's lie at higher field than equatorial and that the two types of equatorial "hinge" CO's are not very different. Then, if the difference in $\delta(^{13}C)$ for equatorial and axial is about the same as for the isoelectronic compound IV, "hinge" assign-

(12) There are two crystallographically independent molecules.[5]
(13) Gas evolution was measured using a gas microvolumeter: Davis, D. D.; Stevenson, K. L. *J. Chem. Educ.* **1977**, *54*, 394.
(14) Housecroft, C. E.; Fehlner, T. P. *J. Am. Chem. Soc.* **1986**, *108*, 4867.
(15) Vites, J. C.; Housecroft, C. E.; Jacobsen, G. B.; Fehlner, T. P. *Organometallics* **1984**, *3*, 1591.
(16) Hong, F.-E.; Rath, N.; Fehlner, T. P., unpublished observations.
(17) Tachikawa, M.; Muetterties, E. L. *J. Am. Chem. Soc.* **1980**, *102*, 4541.

ments can be made as shown in Figure 7. These three resonances average to δ 214.5 vs. the observed value of δ 214.8 at 20 °C. Localized CO exchange at a metal center associated with a bridging hydrogen atom is known to have a higher barrier than that at an unbridged metal.[18] Hence, the assignment of the bridged "wing-tip" $Fe(CO)_3$ group to the resonances at δ 223 and 212 is reasonable. This leaves the resonance at δ 216 for the three CO's on the other "wing-tip" requiring intrametal site exchange at this iron to be still rapid at −60 °C. The loss of intensity of this resonance in going to −80 °C suggests incipient freezing out of this site exchange. With these assignments the calculated 20 °C average "wing-tip" resonance is 217.5 vs. an observed value of δ 217.8. Note, that the important observations, viz., rapid localized site exchange of CO's with rapid H exchange at 20 °C and no H exchange at the lowest temperature, are independent of the detailed assignment.

The fluxional behavior of II is significantly different from that of IV. The ^1H NMR of IV shows no exchange of the two types of protons at room temperature[19] while the ^{13}C NMR in the carbonyl region shows only four types of CO at −80 °C (2:4:4:2). This shows that a low barrier path for FeHC proton exchange between the two carbon wing-tip sites not involving the FeHFe hydrogen must exist. Therefore, there must be two H exchange processes operative in IV: one that scrambles FeHFe and FeHC and one that exchanges the FeHC proton between the two Fe(wing)–C sites. The former process may be described as movement of the proton over the cluster surface whereas the latter may well be the simple "flipping" of the proton between the two sites. Although movement of the proton over the cluster surface is more facile for the borane derivative, the proton "flip" is clearly less facile in the metallaborane. The difference lies in the relative strengths of the interaction of the endo hydrogen with the metal framework compared to the interaction with the main-group atom. The proton "flip" in which the main-group-H bond is retained and metal–H bond broken will be favored by strong main-group–H interactions (and weaker metal–H interactions), viz., in the carbon derivative IV. The processes whereby the hydrogen wanders over the metal framework are enhanced by both stronger metal–H and weaker main-group–H interactions, viz., in the boron derivative.

Phosphine Substitution. Modifying the cluster charge distribution is one obvious way of perturbing endo hydrogens. Replacement of exo-CO ligands with phosphines constitutes a method for increasing electron density at the substituted metal. Examples of endo-hydrogen rearrangement on tetrametal clusters caused by phosphine substitution are known.[20] Our interest lies in determining whether such an approach will induce endo-hydrogen movement on a main-group–transition cluster.[4] As reported earlier,[14] the reaction of a hydrogen-rich Fe_3 ferraborane (III) with a phosphine resulted in extensive cleavage of the cluster and H_2 elimination. Compound II appears more robust with respect to fragmentation which may reflect larger cluster size and/or lower hydrogen content. It has been shown that IV undergoes monosubstitution with a variety of phosphine ligands at the wing-tip hydrogen-bridged iron atom.[21] The course of the reaction of II with less than 1 mol equiv of $PPhMe_2$ as followed by ^{11}B NMR is shown in Figure 8. The major product has a boron chemical shift of δ 141.7, but the formation of this product is accompanied by an intermediate with δ (^{11}B) 126. The time dependencies of the ^{11}B signals at high phosphine levels shown in Figure 9 strongly suggest that this intermediate precedes the formation of the primary product. Addition of another mole equivalent of the phosphine leads to the production of a product with δ(^{11}B) 117.9

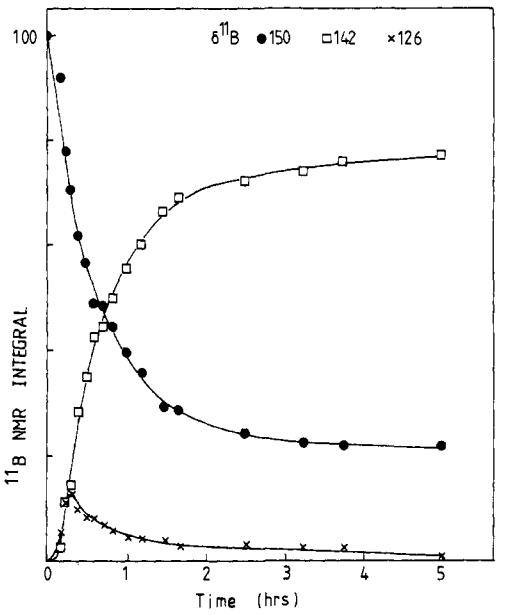

Figure 8. ^{11}B NMR integrals of II (●), V (□), and the intermediate δ 126 (×) as a function of time for the reaction of 0.070 mmol of II with an equivalent amount of $PhMe_2P$ in CH_2Cl_2 at 30 °C.

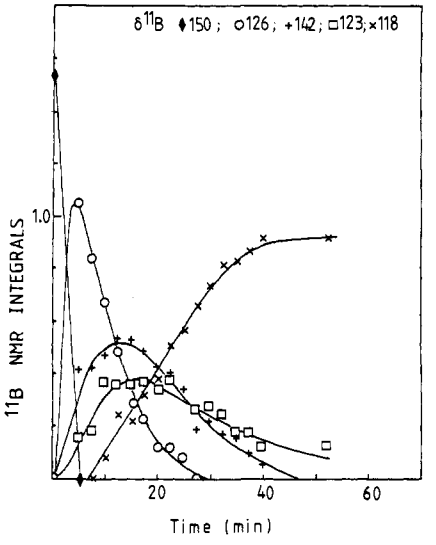

Figure 9. ^{11}B NMR integrals of II (♦), intermediate δ 126 (○), V (+), intermediate δ 123 (□), and VI (×) as a function of time for the reaction of II with a 120-fold excess of $PhMe_2P$ in $CD_3C(O)CD_3$ at 30 °C.

via an intermediate with δ(^{11}B) 123 in a manner similar to Figure 8 but about 5 times more slowly. The entire sequence of events is illustrated in Figure 9 which shows the time dependence of the composition of a system containing II and a large excess of phosphine. The overall rate of substitution is much higher showing dependence on phosphine concentration, and the time dependencies of the products are consistent with the reaction sequence: δ 150 → δ 126 → δ 142 → δ 123 → δ 118.

The nature of the two stable products, δ 142 and 118, is revealed by spectroscopic studies (see experimental section). These data suggest that the products are the anions V and VI, i.e., the singly and doubly substituted derivatives of II. The former appears to exist as a single isomer, and the ^{11}B and ^1H chemical shifts are similar to those observed for the unsubstituted ferraborane suggesting similar structure. In addition, the FeHFe–FeHB scrambling process that was rapid at room temperature in the unsubstituted ferraborane is now slow on the NMR time scale.[4] The increase in the kinetic barrier is attributed to a stabilization of one of the protons by phosphine substitution (see below). A single ^{31}P NMR resonance is observed at a chemical shift characteristic of $PPhMe_2$-substituted iron carbonyl clusters.[14,22] Substitution

(18) Rosenberg, E.; Thorsen, C. B.; Milone, L.; Aime, S. *Inorg. Chem.* **1985**, *24*, 231.

(19) Spin saturation experiments at high temperature show that exchange is occurring: ref 17.

(20) Shapley, J. R.; Richter, S. I.; Churchill, M. R.; Lashewycz, R. A. *J. Am. Chem. Soc.* **1977**, *99*, 7384.

(21) The consequences of phosphine substitution on the exchange processes of $HFe_4(CO)_{12}CH$ have been explored. Muetterties, E. L.; Geerts, R. L.; Tachikawa, M.; Burch, R. R.; Sennett, M. S.; Williams, J.; Beno, M. *Abstr. Pap.—Am. Chem. Soc.* **1982**, *182nd*, INORG 89. Wadepohl, H.; Muetterties, E. L.; Day, V. W. *GdCh. 20th Hauptversammlung*, Heidelberg, 1985.

Chart II

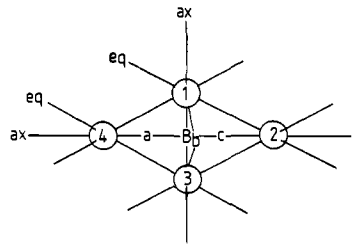

at a "wing-tip" position is supported by the fact that $^{31}P-^{1}H$ coupling is observed with the FeHB proton but not with the FeHFe proton. The estimated magnitude of the coupling constant suggests equatorial substitution, i.e., cis to the hydrogen atom.[22,23] The methyl ^1H resonance is a doublet, and this is consistent with either axial substitution or equatorial (Chart II) substitution combined with a fluxional process whereby the phosphine ligand passes through a plane of symmetry. The ^{13}C NMR resonance of the methyl carbon exhibits P–C coupling at 20 °C, but the resonance becomes broad at −80 °C. Hence, all these observations are consistent with equatorial phosphine substitution combined with a rapid intramolecular fluxional process at the substituted iron site. The ^{13}C NMR in the CO region is consistent with this interpretation. At 20 °C three carbonyl resonances are observed rather than the two exhibited by the unsubstituted compound, i.e., one resonance due to two equivalent "hinge" $Fe(CO)_3$ fragments with rapid localized site exchange (still somewhat broad, however), one resonance due to a "wing-tip" $Fe(CO)_3$ with rapid localized site exchange, and one resonance due to a substituted "wing-tip" $Fe(CO)_3$ with rapid localized site exchange. The substituent shifts agree with previous work on related systems in which it was demonstrated that phosphine substitution causes a downfield shift in the ^{13}C NMR of about 5 ppm for the CO's on the substituted metal and a smaller downfield shift for the other CO's.[22] At −80 °C the ^{13}C NMR exhibits one sharp signal at δ 218.0 which is assigned to the three CO's at the unsubstituted (non-H-bridged) wing-tip iron. The fact that all other signals are still broad at this temperature is also reasonable as phosphine substitution at a "wing-tip" iron atom reduces the barrier of localized site exchange at adjacent metal sites[24] (viz., "hinge" atoms).

The second stable substitution product VI is anionic, contains two phosphines (by ^{31}P NMR integrals with respect to PPN cation), and exhibits both ^{11}B and ^1H NMR chemical shifts similar to those of neutral I with the exception that no FeHFe proton is observed from −90 to 20 °C. In addition, the line-narrowed, proton-coupled ^{11}B resonance is a partially resolved triplet. Thus, in contrast to the unsubstituted and monosubstituted compounds, endo-hydrogen rearrangement has accompanied the addition of the second phosphine. Assuming that the preference for "wing-tip" substitution established in the monosubstituted derivative also holds for VI and that disubstitution at a single metal site is sterically unlikely,[25] the ^{31}P NMR data point toward "wing-tip–wing-tip" substitution. A single ^{31}P NMR resonance is observed at 20 °C and splits into two signals of equal intensity at low temperature. This is consistent with equatorial substitution combined with rapid intrasite exchange at 20 °C and freezing out to the "cis" and "trans" isomers at reduced temperatures. Hence, VIa (defined as "cis" in Chart I) and VIb ("trans") are the structures postulated for the disubstituted product.

In contrast to the two stable products, only a fragmentary picture of the two intermediates is revealed by this work. Information available is limited to the time dependence of concentrations (Figures 8 and 9), ^{11}B chemical shifts, calculated

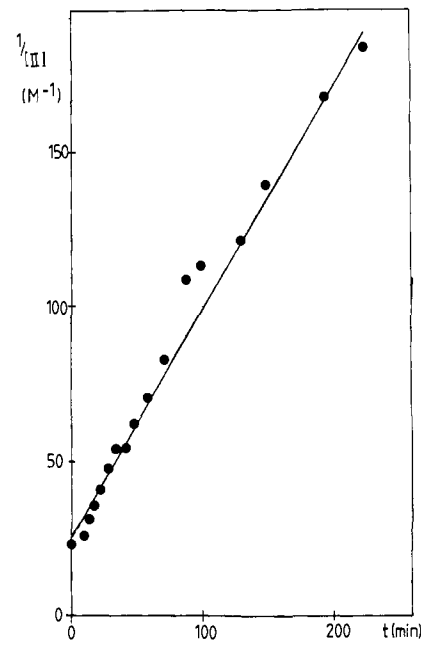

Figure 10. Second-order plot of $1/[II]$ vs. t for the reaction of a 1:1 mole ratio of II to $PhMe_2P$ in CH_2Cl_2 at 30 °C.

Table II. Observations on the Kinetic Parameters for the Products of the Substitution of II by $PhMe_2P$

$[PhMe_2P]_0$, M	$[II]_0$, M	k(1st) for δ 126 loss, min^{-1} [coeff of determination]	inducn period for formation of VI	max yield of V, %
0.025	0.028			90
0.31	0.005	0.15 [0.89]	13	45
0.60	0.005	0.14 [0.98]	8	33
0.99	0.005	0.17 [0.95]	5	25

properties, and properties of related compounds. The kinetics of the substitution reaction could not be examined under pseudo-first-order conditions as, with excess ligand, disubstitution was competitive with monosubstitution (Figure 9). However, a first-order plot of the data from Figure 8 was decidely curved while a second-order plot was linear, yielding a rate constant of 0.014 M^{-1} s^{-1} at 30 °C (Figure 10). The data in Table II show that at high ligand levels the rate of decay of δ 126 is independent of ligand concentration. On the other hand, the maximum yield of V (δ 142) decreases with increasing ligand level and the induction period for the formation of VI (δ 118) decreases with increasing ligand level. This is consistent with the stoichiometric reaction mechanism:

$$\text{II } (\delta\ 150) + L \rightarrow \delta\ 126 \rightarrow \text{V } (\delta\ 142)$$

$$\text{V } (\delta\ 142) + L \rightarrow \delta\ 123 \rightarrow \text{VI } (\delta\ 118)$$

That is, II reacts with phosphine in an associative process to produce an intermediate that decays in a unimolecular process to yield the stable monosubstituted product. This sequence is repeated to produce the disubstituted anion. Corroboration of this conclusion results from the following analysis. For a 1:1 mixture of II with $PhMe_2P$, the decay of II in the first 60 min of reaction can be approximated with an exponential decay ($k = 2.0 \times 10^{-2}$ min^{-1}). With use of the measured first-order decay constant for intermediate δ 126 (Table II, Figure 9), the calculated maximum relative yield and time of maximum yield of intermediate δ 126 are 10% and 16 min, respectively, vs. observed values (Figure 8) of 13% and 17 min, respectively. Most likely, intermediate δ 126 is a phosphine adduct of II or a substitutional isomer of V. Intermediate δ 123 probably bears a corresponding relationship to V or VI. If an adduct, the intermediate could either retain the initial Fe_4B core structure A or open up to B. Examples of clusters retaining the "butterfly" structure with 64 electrons

(22) See for example: Fox, J. R.; Gladfelter, W. L.; Wood, T. G.; Smegal, J. A.; Foreman, T. K.; Geoffroy, G. L.; Tavanaiepour, I.; Day, V. W.; Day, C. S. *Inorg. Chem.* **1981**, *20*, 3214.
(23) Stunz, G. F.; Shapley, J. R. *J. Am. Chem. Soc.* **1977**, *99*, 609.
(24) Band, E.; Muetterties, E. L. *Chem. Rev.* **1978**, *78*, 639.
(25) McDonald, W. S.; Moss, J. R.; Roper, G.; Shaw, B. L.; Greatrex, R.; Greenwood, N. N. *J. Chem. Soc., Chem. Commun.* **1969**, 1295.

Chart III

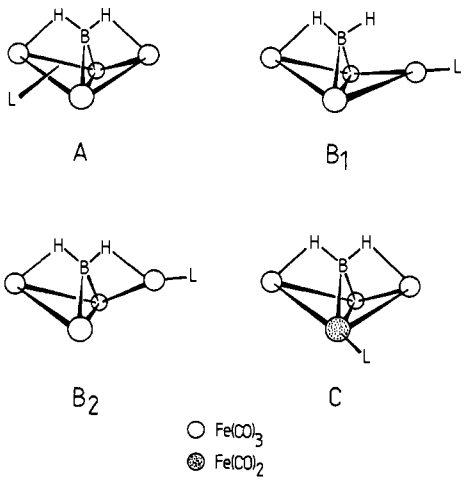

are known albeit with distorted M–M bonds in the cluster framework.[26]

The ^{11}B chemical shifts of the two intermediates are structurally significant. An empirical correlation for ferraboranes, developed independently,[27] shows that increasingly low-field chemical shifts are observed with increasing number of direct metal–boron interactions. More pertinent here is the fact that replacement of an MB interaction by an MHB interaction results in an upfield shift of about 30 ppm. Hence, we suggest that the boron atoms in the two intermediates, δ 126 and 123, have two FeHB interactions as observed in the final disubstituted product VI. In addition, an open intermediate formed by severing a FeB bond ($\mathbf{B_1}$) seems unlikely since the maximum calculated chemical shift (assuming a terminal hydrogen on boron) is δ 90. However, an intermediate formed by cleaving a FeFe bond (B_2) is consistent with the observed boron chemical shift. On the other hand, the calculations show that the LUMO of II has a high metal character with the largest contribution from hinge iron atoms. Hence, nucleophilic attack to produce phosphine substitution at a hinge position, C, followed by cluster rearrangement to produce the "wing-tip" isomer is a viable alternative. This may account for the slowness of the second substitution process relative to the first, i.e., steric hinderence of attack at a "hinge" position.

The conversion of V to VI is accompanied by significant cluster fragmentation with the formation $Fe(CO)_3(PPhMe_2)_2$ and some $Fe(CO)_4(PPhMe_2)$[14] being observed. Hence, not only does phosphine substitution perturb the endo hydrogens, but also it labilizes the cluster towards fragmentation.

Endo-Hydrogen Position and Mobility. The results of extended Hückel calculations are consistent with the spectroscopic information on the identities of the substituted products. Calculated total energies for a reasonable selection of possible isomeric products (supplementary material) show the most stable monosubstituted derivative with one FeHFe and one FeHB to be structure V and the most stable disubstituted compound to be structure VI. However, energy differences between the various isomers are small. The most stable monosubstituted derivative corresponds to placing phosphine on the most positive metal atom in II. Substitution at a "wing-tip" position is favored over "hinge", and equatorial ("wing-tip") is favored over axial substitution. The endo hydrogens appear to be distributed such that the most uniform charge distribution is obtained. That is, the replacement of CO by phosphine, results in an increase in the electron density on the metal substituted, and this increase is moderated by placing an endo hydrogen adjacent to the position of substitution.

The $[HFe_4(CO)_{12}EH]$ cluster, E = C or B^-, possesses two endo hydrogens with stable positions that depend on E as well as the replacement of CO by PR_3. As demonstrated above, replacement of two "wing-tip" CO's with PR_3's for E = B^- results in a change

(26) Adams, R. D.; Yang, L.-W. *J. Am. Chem. Soc.* **1983**, *105*, 235.
(27) Fehlner, T. P., unpublished information.

Table III. Total Energies and HOMO–LUMO Gaps of II as a Function of Substitution

H locans[a]	positn of substitutn[a]	ΔE,[b] eV	ΔHOMO–LUMO,[b] eV
a, b		0.48	0.15
a, c			
a, b	4(eq)	0.49	0.19
a, c	4(eq)		
a, b	2(eq),4(eq)	0.73	0.36
a, c	2(eq),4(eq)		

[a] See Chart II for nomenclature. [b] $\Delta E = E(ac) - E(ab)$.

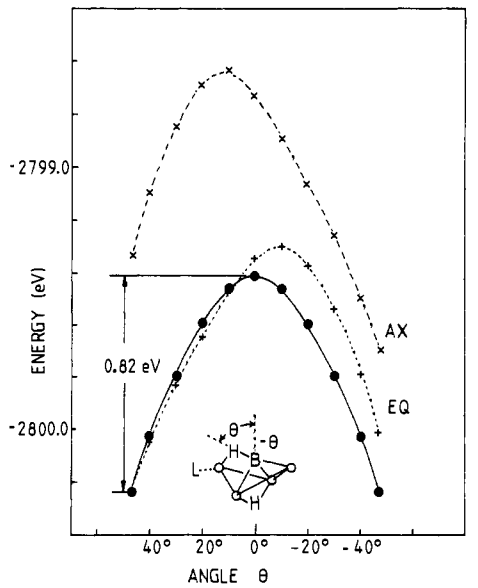

Figure 11. Extended Hückel energies for II (●), V equatorial (+), and V axial (×) as a function of FeHB hydrogen position as defined by the schematic drawing. The total energies of the isomers of V are shown, and that of II has been arbitrarily adjusted for comparative purposes.

in the most stable endo-hydrogen arrangement. In terms of calculated total energy, the calculations predict the most stable arrangement to be the one with two FeHB hydrogens even for the unsubstituted cluster. However, as is shown in Table III, the preference for two FeHB hydrogens increases with increasing phosphine substitution. Although the calculations are predjudiced toward BHFe interactions vs. FeHFe, the observed trend in stabilities as a function of extent of PR_3 substitution is reproduced.

The mobilities of the two endo hydrogens of $[HFe_4(CO)_{12}EH]$ E = C or B^-, also depend on the identity of E. As demonstrated above, FeHE–FeHFe exchange is reduced by replacing B^- with C or one "wing-tip" CO with PR_3 whereas FeHE exchange between the two available FeE edges is enhanced by replacing B^- with C. Because we do not know the mechanisms for the fluxional processes revealed by the NMR observations, we cannot explicitly calculate the reaction barriers. However, insight into the nature of these processes results from an examination of a simple fluxional process as perturbed by changing main group atom and metal ligands. The "test" process chosen is defined in Figure 11 as a simple "flip" of the FeHE proton between the two equivalent FeE edges. The "test" process may well correspond to the mechanism for CHFe exchange in IV at low temperature whereby the "wing-tip" irons are made equivalent. For E = C the calculated barrier is 0.31 eV whereas for E = B^- the barrier is 0.82 eV. The difference in barriers presumably reflects the breaking of a stronger FeH interaction in the latter case as the EH bond is retained in the process. As shown in Figure 11, for either axial or equatorial substitution the overall barrier for the "test" process is increased. Note, however, that the intrinsic barrier is reduced to 0.71 eV for the equatorial isomer. The larger barrier is due to the unequal stabilities of the proton in the two sites resulting from phosphine substitution. Therefore, even though the actual process whereby the endo hydrogens are exchanged must be different, we postulate

that stabilization of the FeHB endo hydrogen by phosphine substitution causes slower exchange in V than in II. The calculated properties suggest a correlation of H location with the charge distribution. The charge distribution depends on the identity of the main-group atom as well as the extent of phosphine substitution for CO. Both C substitution for B^- and phosphine substitution for "wing-tip" CO result in a stabilization of an adjacent endo hydrogen with a consequent reduction in the rate of FeHE–FeHFe exchange.

Experimental Section

General Procedures. All reactions were carried out by using Schlenk techniques.[28] Solvents were dried (toluene over anhydrous $MgSO_4$, hexane over molecular sieve), degassed, and distilled before use; dichloromethane was dried over molecular sieve and degassed before use. The following reagents were used as received: PPNCl (bis(triphenylphosphine)nitrogen(1+) chloride) (Aldrich), $PhMe_2P$ (Aldrich), BH_3·THF (Aldrich, 1.0 M was titrated before use),[29] $(C_2H_5)_3BHLi$(Aldrich), $Fe_2(CO)_9$ (Aldrich), $Fe(CO)_5$ (Aldrich), and H_3PO_4 (Fisher, 85%). Column chromatography was performed on 60–200 mesh silica gel (Baker). ^{11}B, ^{31}P, ^{13}C, and ^1H FT NMR spectra were recorded on a Nicolet 300-MHz spectrometer. ^{11}B chemical shifts are reported with respect to $\delta(BF_3{\cdot}OEt_2)$ 0, ^{31}P shifts with respect to $\delta(H_3PO_4)$ 0, and ^{13}C and ^1H shifts with respect to δ (Me_4Si) 0. ^{11}B NMR integrals were measured against an external standard of $[B_3H_8]NBu_4$ in acetone-d_6 which itself was calibrated against a solution of BH_3·THF of known concentration. Uncorrected ^{11}B NMR integrals were used as a quantitative measure of reactants and products. Infrared spectra were recorded on a Perkin-Elmer 983 spectrometer. The Beer's law plots for the determination of $Fe(CO)_5$ were based on the 2000 and 2020 cm^{-1} absorptions and were linear over the concentration range, $(1.2 - 15.0) \times 10^{-3}$ M. A Carle Model 311 gas chromatograph with molecular sieve and porapak columns in series and argon as a carrier gas was used to qualitatively identify evolved gases. Volumetric gas measurements were carried out with an adaptation of a previously described microvolumeter.[13] The Mössbauer effect spectrum was obtained at 78 K on a conventional constant acceleration spectrometer which utilized a room-temperature rhodium matrix cobalt-57 source and was calibrated at room temperature with natural abundance α-iron foil. The spectrum was fit to Lorenzian line shapes by using standard least-squares computer minimization techniques. [III]PPN was prepared as reported previously.[30]

Preparation of I. To 2.5 mmol of $Fe_2(CO)_9$ in 20 mL of hexane in a 250-mL round-botton flask at 0 °C was added 5 mmol of $Fe(CO)_5$ with vigorous stirring followed by 6 mmol of $LiHB(C_2H_5)_3$. After 10 min, 10 mmol of BH_3·THF was slowly added with stirring. This was followed by sonication[31] at 25 °C for 5 min, or until all the $Fe_2(CO)_9$ was consumed. The solvents were removed under vacuum, and the residue was protonated with 40% H_3PO_4 (25 mL) and extracted with hexane. Removal of the solvent and the $B_2H_6Fe_2(CO)_6$ byproduct under vacuum resulted in a yield (by NMR) of 0.9 mmol of I. This product is contaminated with $Fe_3(CO)_{12}$ and other hydrocarbyls, but separation is achieved by column chromatography on silica gel with toluene as an eluent. Net yield depends strongly on column size (some deprotonation of I occurs on the column): however, with short columns (3 cm diameter × 10 cm length) yields of pure I of 0.3 mmol are obtained.

Preparation of [II]PPN. [II]PPN or [II][HNR_3] is conveniently produced in quantitative yield by the deprotonation of I via treatment of a hexane solution of I with either methanolic PPNCl or neat amine. However, an alternative and rational route is via [III]PPN. In a typical reaction, 0.02 mmol of [III]PPN in 1.5 mL of toluene/dichloromethane (13:2) was added to solid $Fe_2(CO)_9$ (0.0146 g, 0.04 mmol) and was stirred at room temperature. During the 40-min reaction period, the solution changed from orange-red to an intense brown color and all the solid $Fe_2(CO)_9$ was consumed. ^{11}B and ^1H NMR showed the formation of [II]PPN in better than 90% yield: ^{11}B NMR ($CD_3C(O)CD_3$, −25 °C) δ 150.0 (br, fwhm = 180 Hz; $\{^1H\}$, fwhm = 100 Hz, J_{BH} = 86 Hz);[32] ^1H NMR ($CD_3C(O)CD_3$, −30 °C) δ 7.77–7.58 (m, 30 H, PPN^+), −8.5 (br, 1 H, FeHB), −24.9 (s, 1 H, FeHFe);[33] ^{13}C NMR (CH_2Cl_2, −80 °C) δ 222.5, 217.7, 216.6, 216.0, 211.7, 209.1 (all s, CO), 132–125 (PPN); IR (acetone, cm^{-1}) ν_{CO} 2060 w, 2040 w, 2003 vs, 1983 vs, 1955 m, 1932 m, $\nu_{\text{interstitial B}}$ 808 w.[10] Treatment of a solution of [II]PPN (0.020 mmol in 1.5 mL of toluene) with 0.015 mL of CF_3COOH in an NMR tube with an external $B_3H_8^-$ reference resulted in the production of I in 88% yield (by ^{11}B integrals).

Preparation of $[HFe_4(CO)_{11}(PhMe_2P)BH]PPN$. In a typical preparation a solution of $PhMe_2P$ (0.009 mL, 0.07 mmol) in CH_2Cl_2 or acetone (0.5 mL) was added to [II]PPN (0.07 mmol) in 2.0 mL of the same solvent. Reaction was complete within 6 h at 30 °C, and the yield of $[HFe_4(CO)_{11}(PhMe_2P)BH]PPN$ was 90% by NMR: ^{11}B NMR ($CD_3C(O)CD_3$, 20 °C) δ 141.7 (br, fwhm = 180 Hz, $\{^1H\}$, fwhm = 140 Hz, J_{BH} = 65 Hz);[32] $^{31}P\{^1H\}$ NMR ($CD_3C(O)CD_3$, −80 °C) δ 30.0 (m, 1 P, $\{^1H\}$ selective, J_{PH}(FeHB) = 12 Hz, $PhMe_2P$), 21.7 (s, 2 P, PPN^+); ^1H NMR ($CD_3C(O)CD_3$, 0 °C) δ 7.7–7.5 (m, 35 H, PPN^+ and $PhMe_2P$), 1.89 (d, 6 H, $PhMe_2P$, J_{PH} = 9 Hz), −8.4 (br, 1 H, FeHB), −23.8 (s, 1 H, FeHFe); ^{13}C NMR (CH_2Cl_2, 20 °C) δ 224.4 (2 C), 219.7 (3 C), 218.7 (6 C) (all CO), 132–125 (PPN, $PhMe_2P$), 20.5 (d, J_{PC} = 24 Hz, $PhMe_2P$); IR (CH_2Cl_2, cm^{-1}) ν_{CO} 2048 w, 2034 w, 2004 sh, 1985 vs, 1977 vs, 1950 s.

Preparation of $[Fe_4(CO)_{10}(PhMe_2P)_2BH_2]PPN$. A solution of $PhMe_2P$ (0.0094 mL, 0.07 mmol) in CH_2Cl_2 (0.5 mL) was added to $[HFe_4(CO)_{11}(PhMe_2P)BH]PPN$ (0.07 mmol) in CH_2Cl_2 (2.0 mL). Reaction was 85% complete in 7.5 h at 30 °C; however, about 20% cluster fragmentation accompanied substitution as evidenced by the formation of $Fe(CO)_4(PhMe_2P)$, $Fe(CO)_3(PhMe_2P)_2$:[14] ^{11}B NMR ($CD_3C(O)CD_3$, 20 °C) δ 117.9 (br, fwhm = 210 Hz, line narrowed, br t, J_{BH} = 53 Hz,[32] $\{^1H\}$ fwhm = 175 Hz); ^1H NMR ($CD_3C(O)CD_3$, −60 °C) δ 7.7–7.5 (m, 40 H, PPN^+ and $PhMe_2P$), 1.90 (s, 12 H, $PhMe_2P$), −11.6 (br, 2 H);[31] $^{31}P\{^1H\}$ NMR ($CD_3C(O)CD_3$, 20 °C) δ 31.0 (s, 2 P) [δ 31.9 (s, 1 P), 32.3 (s, 1 P) at −90 °C], 21.7 (s, 2 P, PPN^+). Note: ^1H integrals corrected for contributions due to known fragmentation products using the ^{31}P data.

Extended Hückel Calculations. Calculations were performed by using an idealized cluster geometry derived from the experimental parameters of I.[9,34] PH_3 (d_{PH} = 1.42 Å, d_{FeP} = 2.24 Å, and HPH and FePH angles of 90° and 125.3°, respectively) was used to mimic the $PhMe_2P$ ligand in the substituted derivatives.[35] The extended Hückel calculations[36] employed Slater functions, and the orbital exponents and diagonal matrix elements used are listed in the supplementary material. The arithmetic mean Wolfsberg–Helmholtz approximation with K = 1.75 was used.

Acknowledgment. We gratefully acknowledge the support of the National Science Foundation (CHE 84-08251) (T.P.F.) and the donors of the Petroleum Research Fund, administered by the American Chemical Society (G.J.L.). We also thank Dr. N. Rath for improvements in preparative procedures and Dr. H. Wadepohl for communicating the results referred to in ref 21.

Supplementary Material Available: Tables showing Hückel total energies and Mulliken charges for selected substitutional isomers and parameters used in the calculations (3 pages). Ordering information is given on any current masthead page.

(28) Shriver, D. F. *The Manipulation of Air Sensitive Compounds*; McGraw-Hill: New York, 1969.
(29) Brown, H. C. *Organic Syntheses Via Boranes*; Wiley: New York, 1975.
(30) Vites, J. C.; Housecroft, C. E.; Eigenbrot, C.; Buhl, M. L.; Long, G. J.; Fehlner, T. P. *J. Am. Chem. Soc.* **1986**, *108*, 3304.
(31) L & R Manufacturing Co. Model 210.
(32) J_{BH} estimated from line width analysis.
(33) The metal hydride resonance actually integrates to 0.2 H. However, low MH integrals are not uncommon: Crabtree, R. H.; Segmuller, B.; Uriarte, R. J. *Inorg. Chem.* **1985**, *24*, 1949.
(34) Fehlner, T. P.; Housecroft, C. E.; Scheidt, W. R.; Wong, K. S. *Organometallics* **1983**, *2*, 825.
(35) Kostic, N. M.; Fenske, R. F. *Organometallics* **1982**, *1*, 489.
(36) Hoffmann, R. *J. Chem. Phys.* **1963**, *39*, 1397.